

The Luminosity of SN 1999by in NGC 2841 and the Nature of 'Peculiar' Type Ia Supernovae

Peter M. Garnavich^{1,2}, Alceste Z. Bonanos^{1,3}, Saurabh Jha¹, Robert P. Kirshner¹, Eric M. Schlegel¹, Peter Challis¹, Lucas M. Macri¹ Kazuhito Hatano^{4,5}, David Branch⁴, Gregory D. Bothun⁶, and Wendy L. Freedman⁷

ABSTRACT

We present *UBVRI* photometry and optical spectroscopy of the 'peculiar' type Ia supernova 1999by in NGC 2841. The observations began six days before visual maximum light which is well-defined by daily observations. The light curves and spectra are similar to the prototypical subluminous event SN 1991bg. We find that maximum light in *B* occurred on 1999 May 10.3 UT (JD 24501308.8±0.3) with $B = 13.66 \pm 0.02$ and a color of $B_{max} - V_{max} = 0.51 \pm 0.03$. The late-time color implies minimal dust extinction from the host galaxy. Our photometry when combined with the recent Cepheid distance to NGC 2841 (Macri et al. 2001) gives a peak absolute magnitude of $M_B = -17.15 \pm 0.23$, making SN 1999by one of the least luminous type Ia events ever observed. We estimate a decline-rate parameter of $\Delta m_{15}(B) = 1.90$, versus 1.93 for SN 1991bg where 1.10 is typical for 'normal' events. We compare SN 1999by with other subluminous events and find that $B_{max} - V_{max}$ color correlates strongly with decline rate and may be a more sensitive indicator of luminosity than fading rate for these objects. We find a good correlation between luminosity and the depth of the spectral feature at 580 nm, which had been attributed to Si II. We show that in cooler photospheres the 580 nm feature is dominated by Ti II which provides a simple physical explanation for the correlation. Using only subluminous type Ia supernovae we derive a Hubble parameter of $H_0 = 75^{+12}_{-11}$ km s⁻¹ Mpc⁻¹, consistent with values found from brighter events.

Subject headings: supernovae: general—supernovae: individual (SN 1957A, SN 1991bg, SN 1998bp, SN 1999by)—distance scale

¹Harvard-Smithsonian Center for Astrophysics, 60 Garden Street, Cambridge, MA 02138

²Physics Department, University of Notre Dame, Notre Dame, IN 46556

³Wellesley College, Wellesley, MA 02481

⁴Department of Physics and Astronomy, University of Oklahoma, Norman, OK 73019

⁵Department of Astronomy and Research Center for the Early Universe, Univ. of Tokyo, Tokyo, Japan

⁶Physics Department, University of Oregon, Eugene, OR 97403

⁷Observatories of the Carnegie Institution of Washington, 813 Santa Barbara St., Pasadena, CA 91101

1. Introduction

Type Ia supernovae (SNIa) are good distance indicators because they are intrinsically bright and appear to have a relatively small dispersion in maximum brightness. Phillips (1993) showed that a relation between the peak brightness and light curve decline rate improves their utility as distance indicators. This was exploited by Hamuy et al. (1996a), Riess, Press, & Kirshner (1995) and Jha et al. (1999) to measure the Hubble constant. Much more distant SNIa have been used to determine the content of the Universe (Garnavich et al. 1998; Schmidt et al. 1998; Riess et al. 1998, Perlmutter et al. 1999).

SNIa are fairly homogeneous in spectral characteristics and intrinsic color at maximum (Filippenko 1997), but in 1991 two spectroscopically ‘peculiar’ SNIa were discovered (Branch, Fisher, & Nugent 1993). Near maximum light, SN 1991T showed only a weak line Si II 615 nm line when it is normally the strongest feature in the optical band (Phillips et al. 1992; Filippenko et al. 1992a). It also displayed a very slow light curve evolution compared to more typical events and was thought to be more luminous than average. That same year SN 1991bg showed an extremely fast light curve evolution as well as a red color at maximum light and strong Ti II in its spectrum (Filippenko et al. 1992b; Leibundgut et al. 1993). The maximum brightness of SN 1991bg was also estimated to be two magnitudes fainter than normal events. SN 1986G (Phillips et al. 1987) appears to have properties between normal and the extreme case of SN 1991bg. Nugent et al. (1995) showed that the gross spectral variations among all SNIa can be accounted for by simply varying the photospheric temperature which suggests peculiar events are just extreme tails of a continuous distribution.

Since 1991, many more supernovae have been discovered serendipitously and in systematic searches and a handful of supernovae similar to SN 1991T and SN 1991bg have been found and studied. Li et al. (2001) added SN 1999aa as a peculiar sub-class which is similar to SN 1991T well before maximum light, but with significant Ca II absorption not seen in the original. From a volume-limited sample, they find 36% of SNIa are somehow spectroscopically peculiar, although Branch (2001) points out a selection bias that raises the fraction to 45% and casts doubt on the usefulness of the term ‘peculiar’.

Only 16% of all the supernovae in the Li et al. sample were classified as SN 1991bg-like with evidence of Ti II in their spectra. Few such peculiar SNIa have been studied in detail: 1992K (Hamuy et al. 1994), 1997cn (Turatto et al. 1998), and 1998de (Modjaz et al. 2000). Because of their rapid evolution, they are often discovered after maximum brightness. Even more uncommon are SNIa that bridge the gap between ‘normal’ events and the extreme SN1991bg-like explosions. SN1986G (Phillips et al. 1987) is one of these intermediate events, but was highly reddened by dust in its host galaxy. More recently, SN 1998bp (Jha et al. 1998; Jha et al. 2001) appears to fall between the normal and extreme objects.

SN 1999by is another rare example of a peculiar, fast-declining SNIa. It was discovered independently by R. Arbour, South Wonston, Hampshire, England, and by the Lick Observatory Supernova Search (LOSS) on 1999 April 30 (Papenkova et al. 1999). SN 1999by is located in NGC 2841, an Sb galaxy, that has been host to three other supernovae (SN 1912A, SN 1957A, and SN 1972R). An early spectrum by Gerardy & Fesen (1999) showed that SN 1999by was a type Ia event and Garnavich et al. (1999) found line

ratios and Ti II absorption consistent with peculiar SN 1991bg-like supernovae. Adding to its peculiarity, SN 1999by is one of the few SNIa to show significant intrinsic polarization (Howell et al. 2001).

Here, we present detailed photometric and spectroscopic observations of SN 1999by. In addition to its fascination as a peculiar supernova, Hubble Space Telescope (*HST*) has recently studied Cepheid variables in its host galaxy (Macri et al. 2001), which makes SN 1999by useful in defining the distance scale.

2. Observations

2.1. Photometry

Observations of the SN 1999by began six days after discovery with the 1.2m telescope at the Fred L. Whipple Observatory (FLWO). Twenty sets of *UBVRI* images were obtained between 1999 May 6 and June 20 (UT) using the 4-Shooter camera, which consists of four 2048×2048 CCD chips. Images were taken in a 2×2 bin mode with the supernova centered on chip 3. The image scale was $0.64''/\text{pixel}$. Late-time *BVRI* images were obtained at FLWO in 1999 Nov. and Dec.

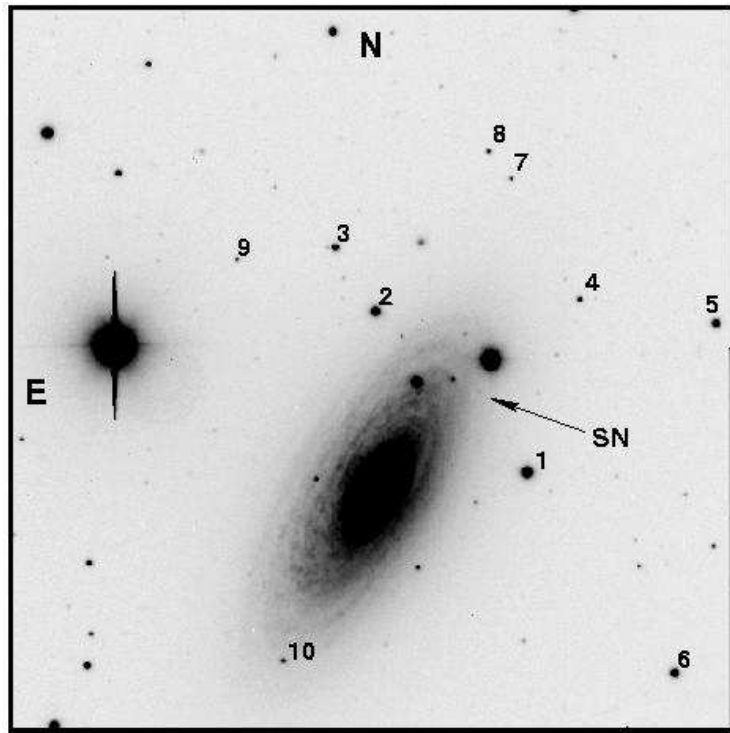


Fig. 1.— The field around NGC 2841 with local comparison stars marked. The field of view is 10.9 by 10.9 arcminutes. The image was taken in 1999 December well after the supernova maximum.

The images were bias corrected and flat fielded using the CCD reduction package in IRAF⁸. We used the DAOPHOT package in IRAF to obtain instrumental magnitudes of the supernova and 10 local standard stars using aperture photometry. Tests using point-spread-function (PSF) fitting photometry showed no difference between the derived magnitudes. SN 1999by went off about 3' from the center of NGC 2841 where there is still significant light contributed by the disk. However, the galaxy is relatively smooth at the resolution of FLWO with only a mild light gradient at the supernova, permitting an accurate local background to be estimated from an annulus around the star. At late times, no contamination from faint stellar sources is seen at the position of the supernova.

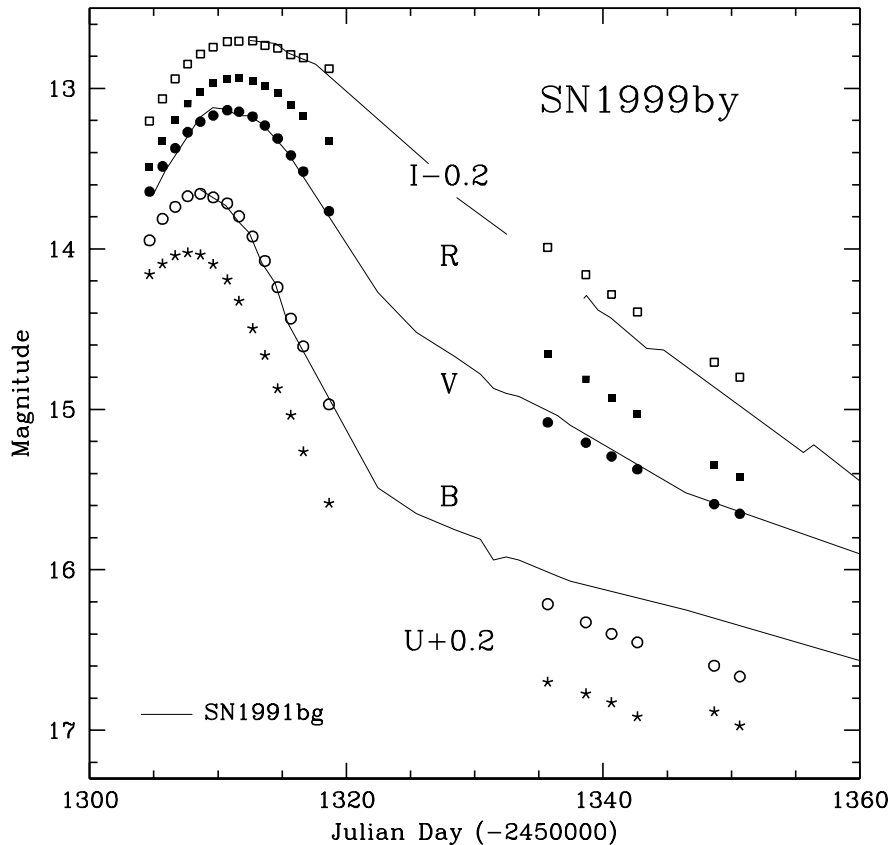


Fig. 2.— Light curves of SN 1999by in the U, B, V, R and I filters. The solid lines show the light curves of SN 1991bg from Leibundgut et al. (1993), with the curves shifted to match the date V -band peak and in magnitude to match the individual light curves near maximum.

Local standard stars were calibrated on four photometric nights at FLWO and two photometric nights at the Vatican Advanced Technology Telescope (VATT). On all those nights Landolt standard stars (Landolt 1992) were observed over a range of airmasses

⁸Image Reduction and Analysis Facility, distributed by the National Optical Astronomy Observatories, which are operated by the Association of Universities for Research in Astronomy, Inc., under cooperative agreement with the National Science Foundation.

allowing for the derivation of linear extinction and color coefficients. The standard magnitudes derived for the local calibrators are given in Table 1 corresponding to the stars marked in the finder chart given in Figure 1. For local calibrators observed on multiple nights, the root-mean-square (RMS) scatter was 0.03 mag. The supernova instrumental magnitudes from May and June were converted to standard magnitudes using local standards stars 1 to 4. The resulting *UBVRI* light curve is provided in Table 2 and displayed in Figure 2. Our standard star calibration has substantially improved over that used by Bonanos et al. (1999) which was based on a single non-photometric night and our *V* maximum is now consistent with that found by Toth & Szabo   (2000).

The light curves for SN 1999by shown in Figure 2 are similar to those of the peculiar type Ia SN 1991bg in their rate of rise and decline from maximum. Although our coverage 20 to 30 days after B_{max} is poor, the *R* and *I* bands appear to lack the prominent ‘second maximum’ seen in normal SNIa.

From the highest-quality image we derive an accurate position for the supernova of 9:21:52.07 51:00:06.54 (2000) based on the *HST* Guide Star Catalog coordinates. Using 14 stars in the field of NGC 2841 for the plate solution we get a scatter of 0.2'' (RMS) which represents the expected accuracy of the astrometry. This is consistent with the positions given by the discoverers (Papenkova et al. 1999).

2.2. Spectroscopy

Spectroscopic observations of SN 1999by were made using the FLWO 1.5 m telescope with the FAST spectrograph using a 300 line/mm grating and a 3'' slit (Fabricant et al. 1998). A majority of the spectra were taken with a single grating setting covering 362 nm to 754 nm. On two nights the observations were done at two grating tilts providing wavelength coverage from 327 nm to 901 nm and three spectra were obtained with a 600 line/mm grating giving twice the resolution but half the typical coverage. Interference fringes were a severe problem at wavelengths longer than 780 nm and could not be completely removed from the data. A total of 18 spectroscopic observations were made between 1999 May 6 (UT) June 22 and a log of the observations is given in Table 3.

We reduced the spectra using IRAF. The two-dimensional CCD exposures were bias and dark corrected and then flat-fielded. Using the APEXTRACT package, we extracted the 1D spectrum at the supernova position, subtracting the sky estimated along two strips parallel to the spectrum. The supernova signal was strong enough that it was used to trace the centroid along the dispersion. Exposures of a HeNeAr lamp taken after each supernova observation were used to calibrate the wavelength. Flux calibration was done by using the exposures of spectroscopic standard stars taken during the night. The spectrograph slit was set at the parallactic angle for both the supernova and the standard star observations to reduce differential slit losses. Not all the observations were done under photometric conditions. Finally, the data were corrected for the Doppler shift due to the radial velocity of NGC 2841 (638 km s⁻¹). The reduced spectra are shown in Figures 3 and 4.

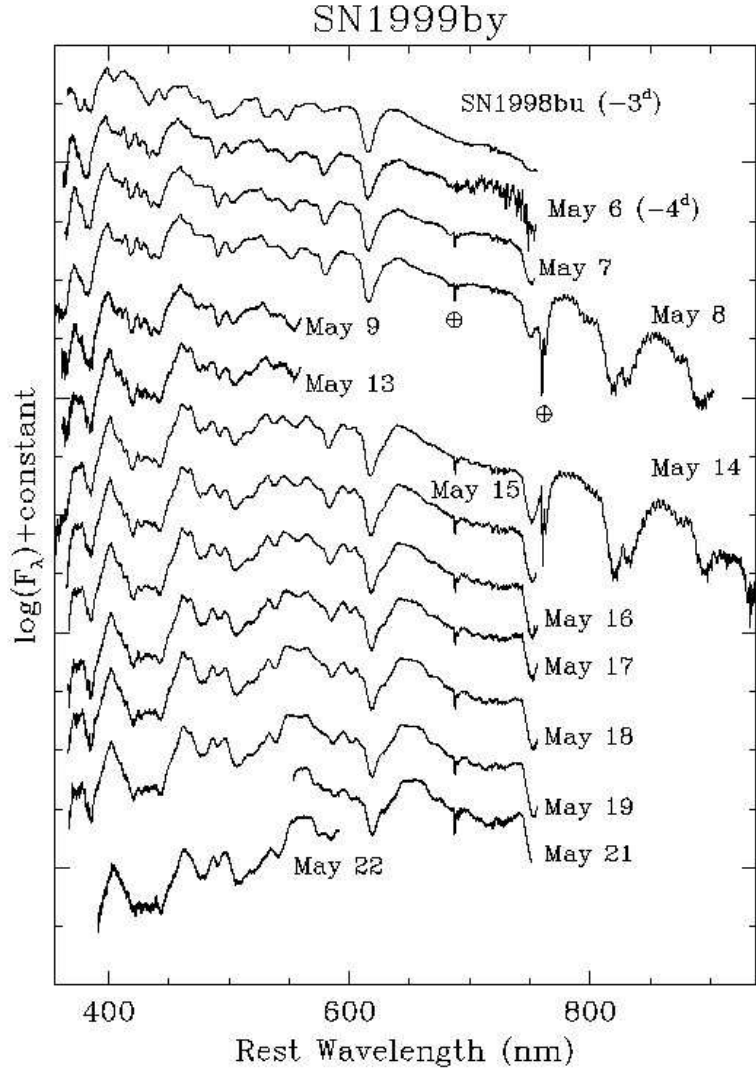


Fig. 3.— Spectra of SN 1999by in May, 1999 from the FLWO 1.5m telescope. For comparison we show the normal but dust reddened SN1998bu three days before maximum light.

3. Discussion

3.1. The Light Curve

The date and magnitude of maximum light in all the filters were estimated by fitting second and third degree polynomials to the May data. Because of the daily sampling, the curves are very well defined and the scatter about the fits was 0.01 mag or less. The results are given in Table 4. A two day difference between the times of B and V maximum is typical of SNIa (Leibundgut 1988) and appears from SN 1999by to be true for fast-declining events as well. The Galactic latitude of NGC 2841 is $+44^\circ$ which means that the extinction through our galaxy is low but not insignificant. The reddening estimate from Schlegel, Finkbinder, & Davis (1998) is $E(B - V) = 0.016$ mag and this correction has been applied in the maximum magnitudes given in Table 5 assuming the standard Cardelli et al. (1989) extinction law.

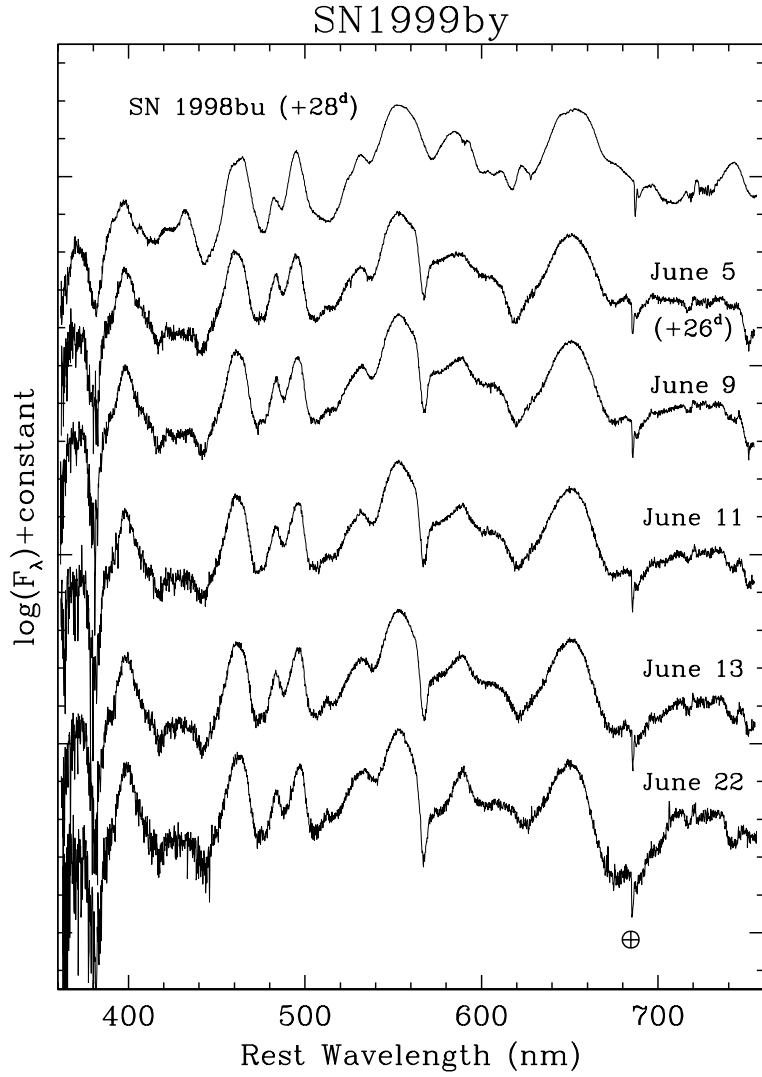


Fig. 4.— Spectra of SN 1999by in June, 1999 during the early nebular stage. For comparison, the top spectrum is that of SN 1998bu at an age of +28 days after B_{max} . The narrow absorption feature seen in SN 1999by near 570 nm is identified as Na I.

The number of magnitudes a supernova fades 15 days after maximum brightness, $\Delta m_{15}(B)$, is a popular way to parameterize a light curve shape. Directly measuring this parameter is difficult from our data because of the Lunar gap starting ten days after B_{max} . It is also dangerous to use the standard template-fitting technique when there are no known SNIa significantly faster than SN 1991bg. Instead, we apply a light curve ‘stretch’ method developed for high-redshift supernovae by Perlmutter et al. (1997). In our implementation, the time axis of the Leibundgut templates (Leibundgut 1988), restricted to $-5 < \text{days} < 15$, are multiplied by a parameter, s , which compresses or expands the light curve mimicking the variation in decline rate. A χ^2 minimization is applied to an observed light curve after correcting for time dilation, where the stretch factor, time of maximum and magnitude of maximum are free parameters. We then applied this technique to the $\Delta m_{15}(B)$ standard templates defined by Hamuy et al. (1996a) as a way to calibrate the stretch factor against $\Delta m_{15}(B)$. Because we are interested in the fast-declining end of the distribution, we added

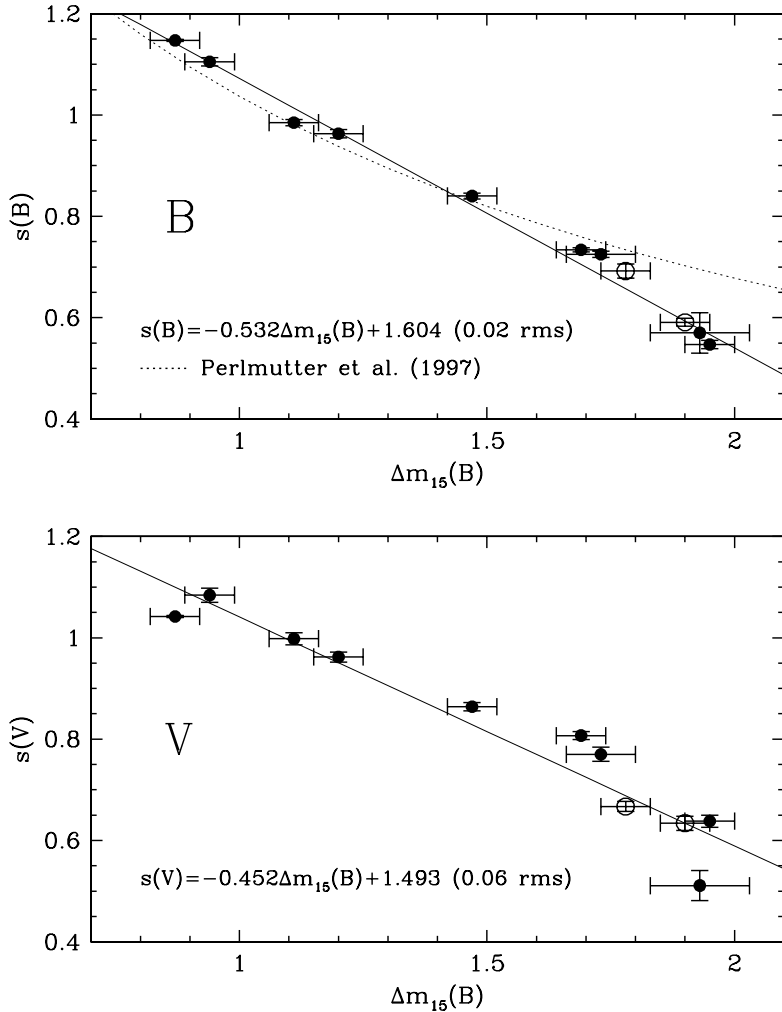


Fig. 5.— The conversion of the stretch parameter, s , to $\Delta m_{15}(B)$. The solid points show the $\Delta m_{15}(B)$ standard SNIa from Hamuy et al. (1996) plus SN1998de from Modjaz et al. (2000). The open points show SN1998bp and the position of SN1999by for its measured stretch. The solid line is the best fit line through the solid points. The dotted line is the conversion of a stretch parameter to $\Delta m_{15}(B)$ from Perlmutter et al. (1997) where the light curve templates were restricted to $\Delta m_{15}(B) < 1.75$.

the well-observed event SN 1998de with $\Delta m_{15}(B) = 1.95 \pm 0.05$ (Modjaz et al. 2000) as a standard light curve.

The calibration between the stretch parameters for B and V and $\Delta m_{15}(B)$ are shown in Figure 5. The conversion of stretch to $\Delta m_{15}(B)$ works best for the B -band with a scatter of only 0.04 mag in $\Delta m_{15}(B)$. Stretch applied to the V -band gives a larger scatter, but consistent results. Direct measurement of the $\Delta m_{15}(B)$ parameter should become slightly non-linear for these very fast-declining events since the first inflection point in the light curve, which signals the onset of the nebular phase, shifts to within 15 days of B_{max} . This

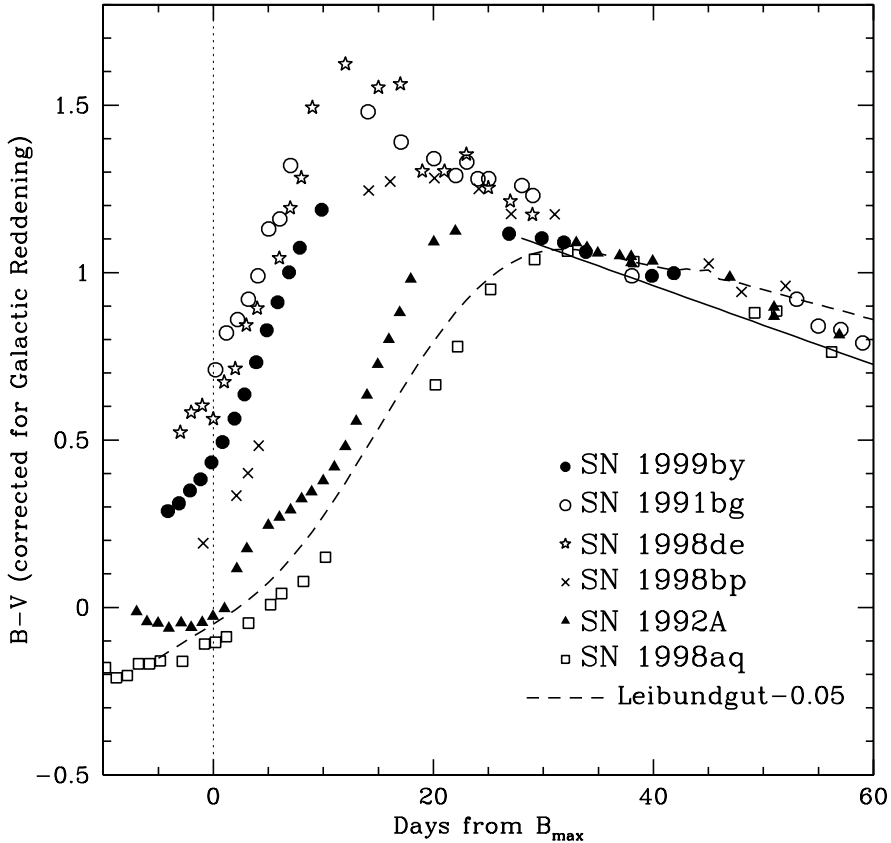


Fig. 6.— $B - V$ color for seven SNIa corrected for Galactic extinction. The solid line is the empirical relation of Lira (1995) for unextinguished supernovae at late-times. The Leibundgut templates have been shifted by 0.05 mag to correct for the average reddening to SNIa from Phillips et al. (1999).

likely contributes to the scatter in Figure 5 but does not have a large effect on our goal of estimating $\Delta m_{15}(B)$ for SN 1999by.

We estimate SN 1999by to have $\Delta m_{15}(B) = 1.90 \pm 0.05$ making it a slightly slower declining light curve relative to SN 1991bg and SN 1998de, but still one of the fastest fading light curves ever observed for a SNIa. For SN 1998bp (Jha et al. 2001), we directly measure $\Delta m_{15}(B) = 1.78 \pm 0.05$, consistent with the derived stretch parameters.

The $B_{max} - V_{max}$ color for SN 1999by is 0.50 ± 0.03 mag which is extremely red compared to normal SNIa (Phillips et al. 1999) which have $B - V < 0.1$. Since the host is a spiral with obvious dust patches, reddening may explain this color. However, other fast declining events appear to be intrinsically red (Leibundgut et al. 1993; Modjaz et al. 2000) near maximum and many of these occurred in elliptical hosts with minimal dust. Figure 6 plots the color curves for SN 1999by compared with other fast-declining events.

Lira (1995) has shown that SNIa with low extinction tend to have the same $B - V$

colors between 30 and 90 days after maximum. This appears to hold for fast-decliners as well, although it has been tested with very few events. This fact has been exploited by Phillips et al. (1999) to correct the brightness of a large sample of SNIa for dust extinction. The Lira relation,

$$(B - V)_o = 0.725 - 0.0118(t_V - 60) \quad (1)$$

is also plotted in Figure 6. The late-time color of SN 1999by is consistent with fast-decliners in ellipticals suggesting insignificant extinction. The average difference between the Lira relation and the late-time supernova color is only 0.014 ± 0.020 , confirming that extinction from the host galaxy is negligible and may indicate that the supernova exploded on the nearside of the NGC 2841 disk.

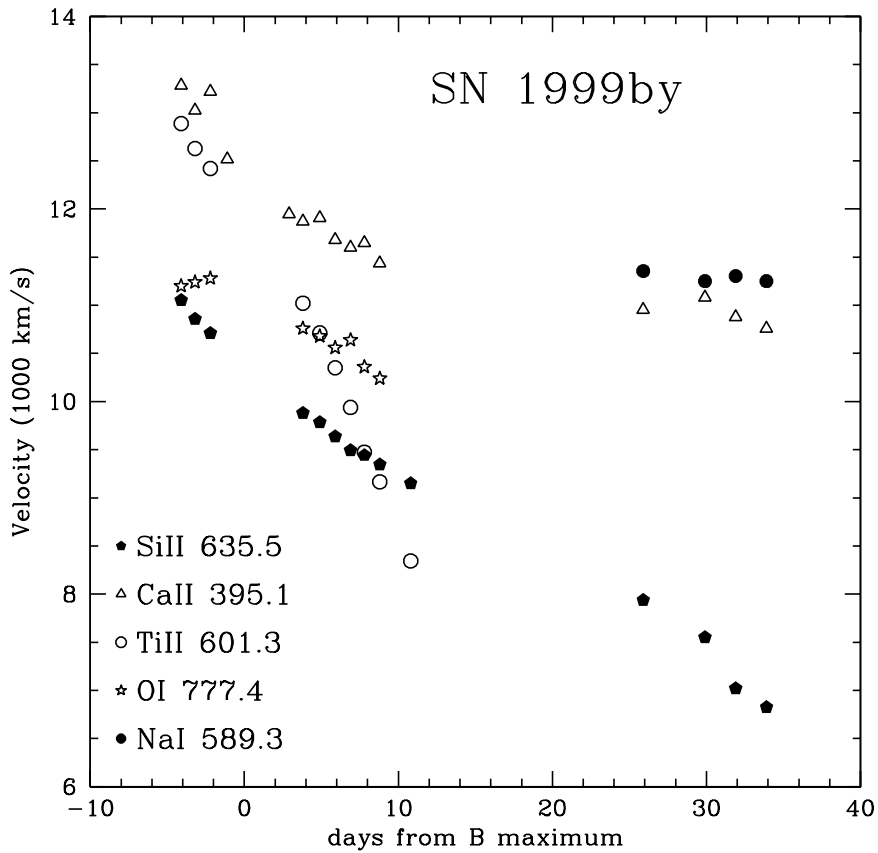


Fig. 7.— Velocities of the Si II 635.5 nm, Ca II 395.1 nm, Ti II 601.3 nm, O I 777.4 nm and Na I 589.3 nm absorption lines in SN 1999by.

3.2. The Spectra

The first spectrum was taken 4 days before B_{max} and the data follow the development without a major interruption until 12 days after maximum.

Comparing the spectrum of SN 1999by at maximum light to spectra of normal SNIa, we see the characteristic Si II feature at 635.5 nm. There is also a prominent absorption band between 420 nm and 440 nm which is unique to fast-declining SNIa. The band as well as absorption at 470 nm and 505 nm were observed in SN 1991bg and have been attributed to Ti II (Filippenko et al. 1992b). The 420 nm band deepens over the observing span but was present even before maximum.

Another feature unique to fast-declining events is the deep O I 777.4 nm line that appears near the edge of the spectral range on most nights. We plot the velocity of O I as measured by the minimum of the absorption trough in Figure 7 along with the velocities derived for other prominent lines such as Si II 635.5 nm, Ca II 395.1 nm and at late-times Na I 589.3 nm. The velocities have been adjusted for the recession velocity of NGC 2841 and a relativistic correction has been applied. Mazzali et al. (1997) found that the O I line in SN 1991bg remained constant at 11000 km s^{-1} for two weeks after maximum light. In SN 1999by, the O I line does decline in velocity from 11200 km s^{-1} before maximum to 10200 km s^{-1} nine days after maximum which is not as steep as for Si II. This may mean the oxygen shell in SN 1999by is deeper than in SN 1991bg.

The velocity of the Si II 635.5 nm absorption versus time is compared with a range of other SNIa in Figure 8. The velocities for the others are taken from Jha et al. (1999, 2001). The Si II velocity before maximum light is similar to normal SNIa, but SN 1999by shows a continual drop in velocity like that of SN 1986G while the typical SNIa levels off at between 11000 km s^{-1} and 10000 km s^{-1} . A steep decline in velocity was also found by Vinkó et al. (2001) for SN 1999by. We find that the average slope around maximum is $130 \text{ km s}^{-1}/\text{day}$ while most normal events have flatter slopes. Only SN 1991bg, with a slope of $160 \text{ km s}^{-1}/\text{day}$, appears to decline faster. Wells et al. (1994) noted a correlation between $\Delta m_{15}(B)$ and Si II velocity decline rate. These data at least show that supernovae with the fastest declining light curves also have the fastest declining Si II velocities after B_{max} .

Comparing the spectra of fast-declining SNIa with more typical events using the time of B_{max} as the reference is not ideal. Better would be to compare the velocities observed in various supernovae using the time of explosion as the zero point. Riess et al. (1999a) find that for a nominal SNIa ($\Delta m_{15}(B) = 1.1$) the interval from explosion to B_{max} is 19.5 ± 0.2 days and this is consistent with SNIa observed at high redshift when a stretch correction is applied based on the light curve shape (Goldhaber et al. 2001). It is therefore possible to approximate the day of the explosion as $t_{exp} = t_{B_{max}} - 19.5 \times s$, where s is the light curve stretch parameter based on the Leibundgut templates. Since s varies by only about 10% for luminous supernovae this provides only a day or two shift in the relative times for the observed velocities. But in SN 1991bg-like events the time of maximum can correspond to as little as 12 days after explosion. In Figure 9 we plot the observed velocities of the Si II absorption in several supernovae versus the time of explosion as estimated above. When the date of explosion is used as the zero point the Si II velocities, SN 1999by and SN 1991bg are always lower than for normal events. Also, the velocities of intermediate supernova, SN 1986G, fall between the extreme fast-decliners and the normal supernovae. For fast-declining events, there appears to be a simple correlation between the light curve shape and photospheric velocity when measured relative to the time of explosion.

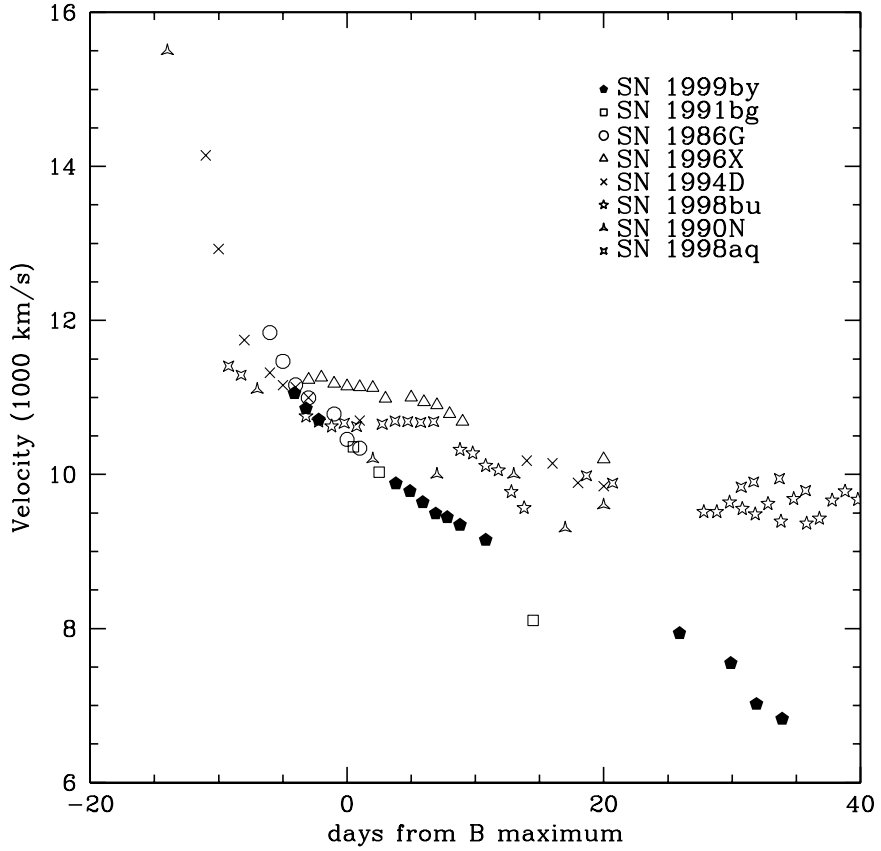


Fig. 8.— Comparison of the Si II 635.5 nm absorption velocity for SN 1999by and other SNIa. While the velocities are similar at maximum, the subluminous supernovae continue to decline in photospheric velocity so at late-times they are distinguishable from more luminous events.

The deep, narrow absorption observed at 567.5 nm in the June spectra (+25 to +35 days) was seen in SN 1991bg and attributed to Na I 589.3 nm by Filippenko et al. (1992b). But models by Mazzali et al. (1997) can not reproduce this feature without adding extra sodium and customizing the distribution to match the small velocity width. If sodium, the velocity in SN 1999by is a constant 11300 km s^{-1} compared to 10500 km s^{-1} in SN 1991bg (Turatto et al. 1996).

We fit models to the SN 1999by spectra using the parameterized spectral synthesis code (SYNOW, Fisher et al. 1999; Hatano et al. 1999a). Figure 10 shows the fit to the May 8 (UT) spectrum taken two days before B_{max} . The fit longward of 420 nm is excellent and shows that most of the features come from Si II, Mg II, Ca II, O I and Ti II. We match the absorption feature near 500 nm with Mg I which has not been identified in a SNIa before. The fit to the May 17 (+7 days) spectrum (Figure 11) shows the Ti II has increased in strength in the blue and the temperature is low enough to allow neutral calcium to appear in the spectrum.

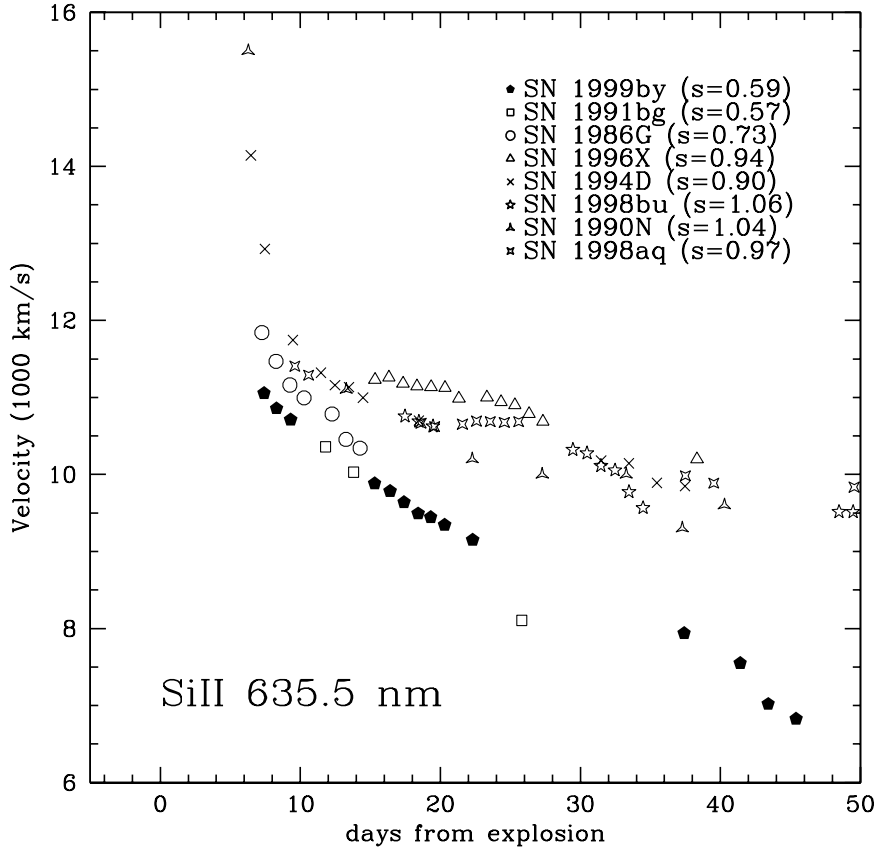


Fig. 9.— Comparison of the Si II 635.5 nm absorption velocity for SN 1999by and other SNIa relative to the time of the explosion. The time of the explosion is estimated from the stretch parameter, s , and the interval 19.5 day interval between explosion and peak brightness for $s = 1$.

A great advantage of SYNOW is that the strength of a single ion can be varied to determine its effect on the entire spectrum. Since Ti II is such an important contributor to the peculiar SNIa spectrum, we plot the variation in Ti II optical depth with a fixed Si II optical depth in Figure 12. The continuum temperature is 12000°K for all the models. The blue region of the spectrum, especially 400-440 nm band is strongly absorbed by the Ti II. Surprisingly an absorption feature at 580 nm appears at high Ti II optical depths. This has commonly been attributed to Si II (e.g. Filippenko 1997) and, indeed it is dominated by Si II 597.9 nm when the Ti II contribution is small. However at low temperatures a number of Ti II lines take over. This nicely explains the correlation between the 580 nm line depth and $\Delta m_{15}(B)$ found by Nugent et al. (1995). They noted a difficulty in physically accounting for the observed increase of the 580 nm to 615 nm depth ratio with decreasing temperature since the ratio of the two lines should mildly decrease with lowering temperature. This is confirmed in Figure 13 which shows the optical depth ratio $\tau(597.9)/\tau(634.7)$ versus temperature from the study of line strengths in supernova atmospheres by Hatano et al. (1999b). The optical depth ratio of the representative Ti II line 601.3 nm to Si II 634.7 nm is also shown and demonstrates a very rapid increase with a

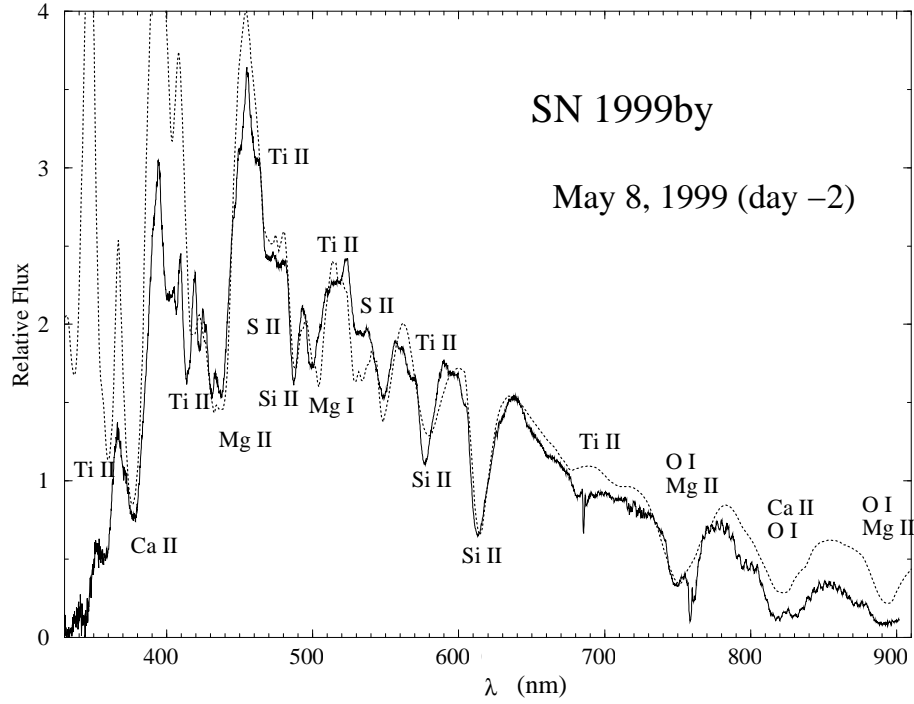


Fig. 10.— A model fit to SN 1999by two days before B_{max} . The solid line is the observed data and the dotted line is the model. Mg I near 500 nm is newly identified in a SNIa.

small temperature drop. We conclude that the 580 nm depth to 615 nm depth ratio, called $\mathcal{R}(\text{Si II})$ by Nugent et al. (1995), is dominated by Si II at high temperatures and Ti II at low temperatures. The rise of the Ti II lines appears to be very rapid as the optical depth relative to Si II increases exponentially with decreasing temperature. This suggests that the ‘peculiar’ SNIa may represent a rather small deviation from normal events but with a rapid line blanketing by Ti II contributing to the red color, the fast B -band decline, the faint B -band luminosity and the unusual spectral characteristics. A more detailed analysis of the effects of Ti II on fast-declining SNIa will be given in Hatano et al. (2001).

The 580/615 nm line depth ratio, which we will now call $\mathcal{R}(\text{Ti II/Si II})$, should still be a useful indicator of decline rate (and intrinsic brightness), at least for the low temperature events. In Figure 14 we plot the $\mathcal{R}(\text{Ti II/Si II})$ for supernovae with a wide range of the $\Delta m_{15}(B)$ parameter, restricting the spectra to within three days of B_{max} . We expect the ratio to be relatively flat with temperature when the 580 nm feature is dominated by Si II and begin to increase when Ti II is present. The rise appears to begin for $\Delta m_{15}(B) > 1.2$, so Ti II is present in the red end of the spectrum even in fast-declining, but normal SNIa. The strong Ti II bands in the blue are probably not apparent for $1.2 < \Delta m_{15}(B) < 1.7$ because the optical depth is much higher there than in the red, but more detailed modelling of this effect is required to confirm this conjecture.

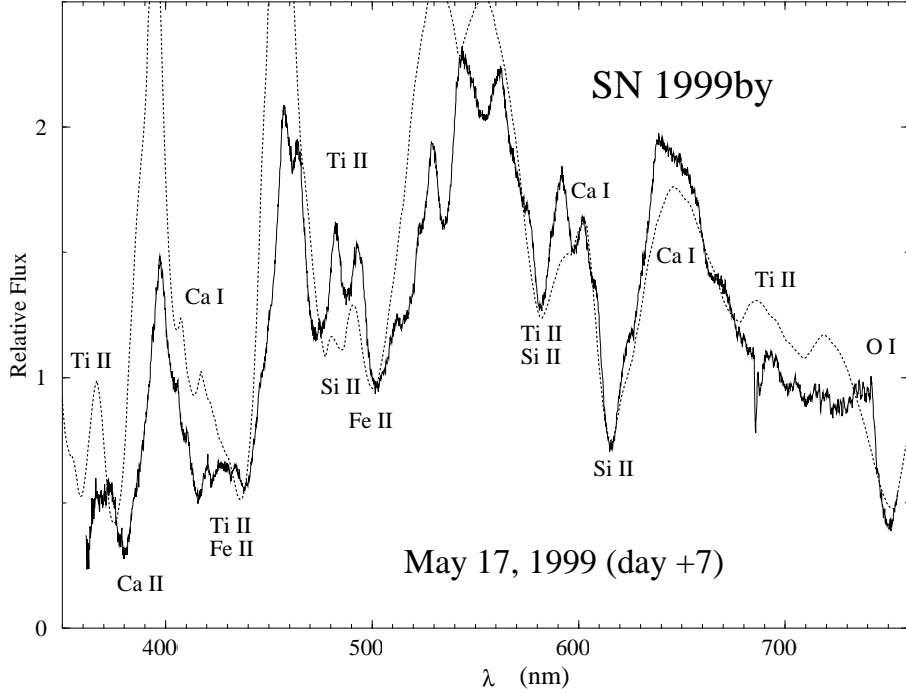


Fig. 11.— A model fit to the observed spectrum of SN 1999by at seven days after B_{max} . The solid line is the observed data and the dotted line is the model. Ca I is identified at a number of locations.

4. Comparison with Other SNIa: What is ‘Peculiar’?

4.1. Color

Peculiar SNIa with fast-declining light curves are defined spectroscopically by the presence of strong Ti II absorption (Branch, Fisher, & Nugent 1993). But we have shown that Ti II is detectable for $\Delta m_{15}(B) > 1.2$, and its strength continuously increases between the ‘normal’ events and the extreme SN 1991bg-like objects. The color of the supernova at maximum may be the best discriminator. Phillips et al. (1999) has shown that the intrinsic $B_{max} - V_{max}$ color of SNIa is less than zero for $\Delta m_{15}(B) < 1.7$. A compilation of fast-declining SNIa is given in Table 5 for events with $\Delta m_{15}(B) > 1.69$. We have left out SN 1992br ($\Delta m_{15}(B) = 1.69$; Hamuy et al. 1996b) and SN 1996bk ($\Delta m_{15}(B) = 1.75$; Riess et al. 1999b) because their light curves are poorly defined. SN 1992K was not discovered until an estimated 12 days after maximum and its parameters are poorly determined but we include it here because it is well established in the literature. The $B_{max} - V_{max}$ color versus $\Delta m_{15}(B)$ for the objects with fast light curves is shown in Figure 15 and demonstrates a sharp break near $\Delta m_{15}(B) \sim 1.7$. Despite the rapid change in slope, the fast-declining events connect well to the end of the ‘normal’ color distribution. No events with $\Delta m_{15}(B) > 1.7$ have been found with blue colors so there remains a monotonic, single-valued function

Evolution of 580 nm feature

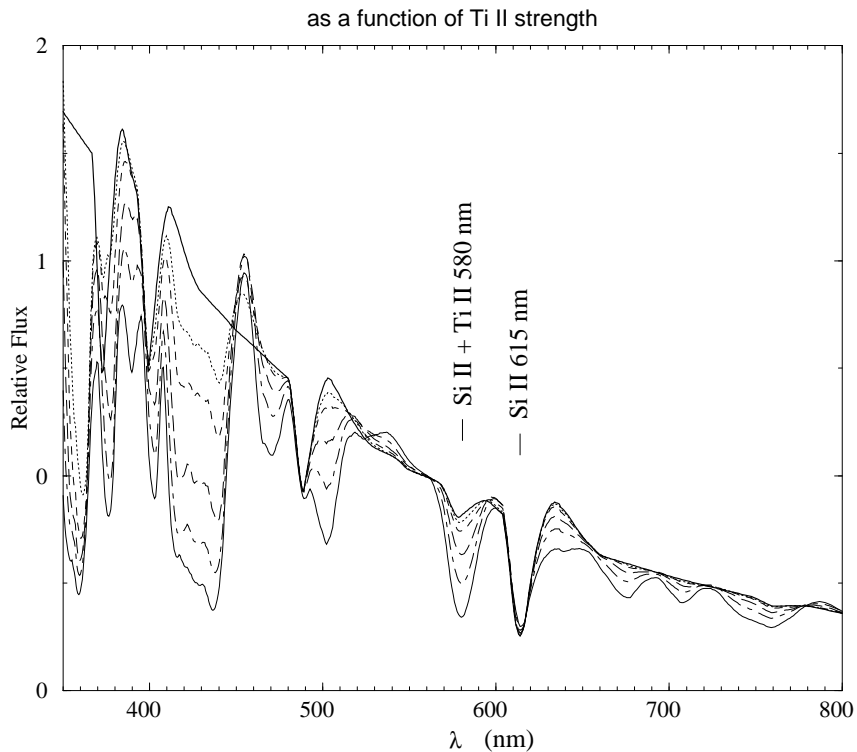


Fig. 12.— A SYNOW model showing only lines of Si II and Ti II on a 12000°K continuum. The optical depth of Ti II is varied with no Ti II shown as the thick solid line. Note the feature at 580 nm, which is normally dominated by Si II, clearly varies with Ti II strength.

connecting light curve shape and color.

4.2. Luminosity

A number of ‘peculiar’ events listed in Table 5 are distant enough to be in the Hubble flow so their luminosities can be compared with normal SNIa. Figure 16 shows the absolute magnitude derived for the peculiar events assuming $H_0 = 72 \text{ km s}^{-1} \text{ Mpc}^{-1}$ (Freedman et al. 2001). The photometric error bars includes an uncertainty of 400 km s^{-1} in the recession velocity due to unknown peculiar velocities of the hosts. SN 1999by is included by using the Cepheid distance of $14.1 \pm 1.5 \text{ Mpc}$ to NGC 2841 from Macri et al. (2001). The normal SNIa are from Phillips et al. (1999) and all magnitudes have been corrected using the reddening estimates from that work. The B -band luminosities show a steep decline toward high $\Delta m_{15}(B)$ which is not well fit by an extension of the Phillips et al. (1999) quadratic fit. Instead, we use an exponential function to match decline rate with luminosity. The best fits for B , V and I are

$$M(B) = -19.338 + 5\text{Log}(H_0/72) + 0.139 \left(\exp[3.441 (\Delta m_{15}(B) - 1.1)] - 1 \right) \quad (2)$$

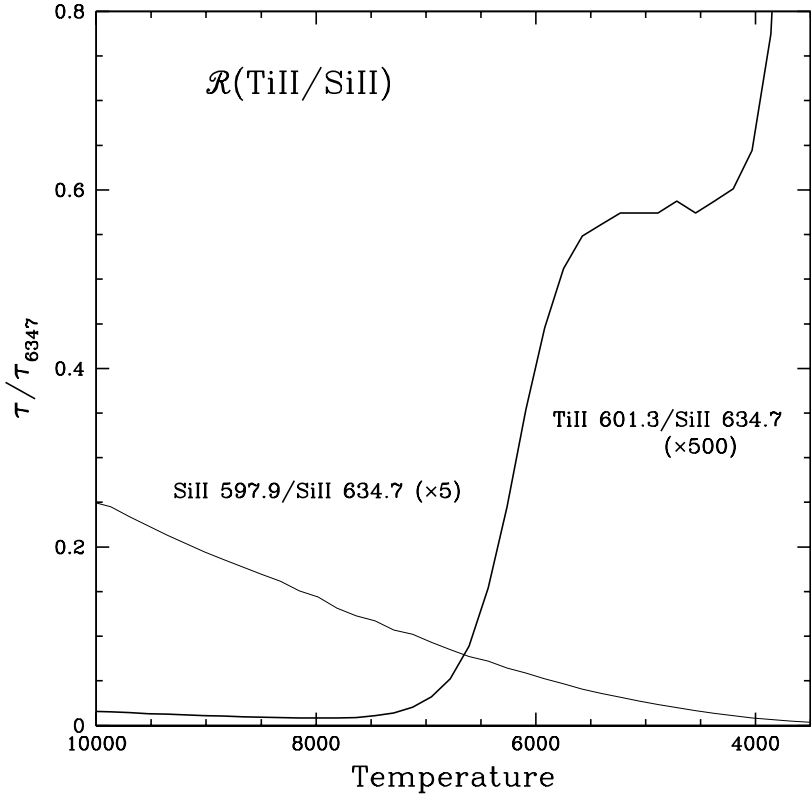


Fig. 13.— Ratio of the optical depth of the Si II line 597.9 nm and Ti II line 601.3 nm to the optical depth of Si II 634.7 nm for a range of temperatures. The optical depths have been multiplied to approximate the observed 580/615 depth ratio. The Si II 597.9 strength is expected to decline relative to Si II 634.7 with decreasing temperature while Ti II begins an exponential rise at 7000°K.

$$M(V) = -19.328 + 5\text{Log}(H_0/72) + 0.096 \left(\exp[3.450 (\Delta m_{15}(B) - 1.1)] - 1 \right) \quad (3)$$

$$M(I) = -18.817 + 5\text{Log}(H_0/72) + 0.060 \left(\exp[3.402 (\Delta m_{15}(B) - 1.1)] - 1 \right) \quad (4)$$

using a χ^2 minimization with three free parameters. Adding an additional linear slope parameter did not improve the overall fit which has an root-mean-squared scatter of 0.19 mag in each band. While this is a larger scatter than obtained when fitting SNIa restricted to $\Delta m_{15}(B) < 1.7$, it shows that normal and peculiar SNIa can be calibrated in a uniform manner and argues for their common origin.

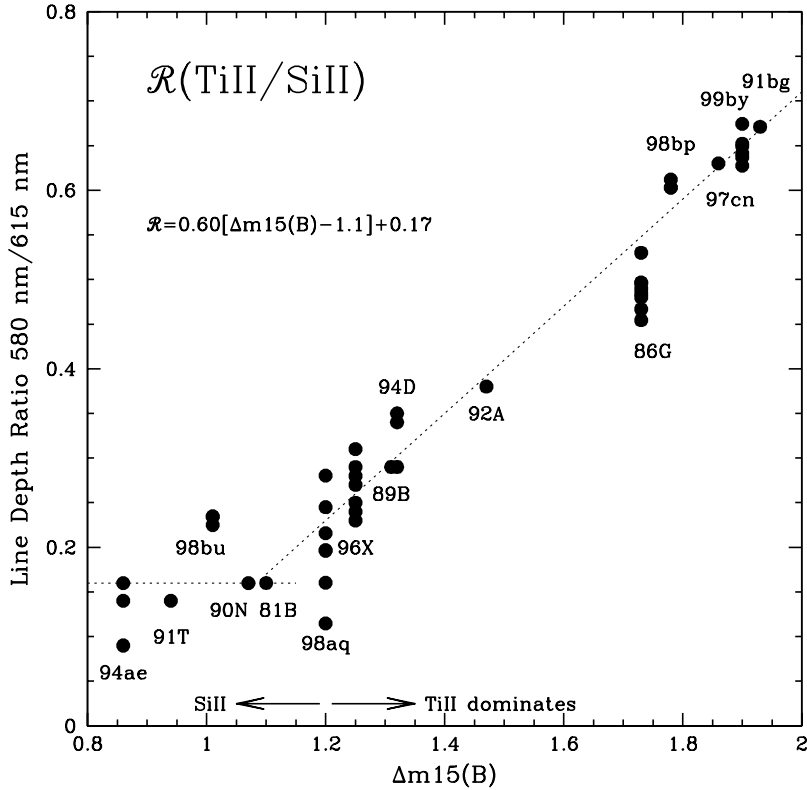


Fig. 14.— Ratio of 580 nm to 615 nm line depth for 15 supernovae. Each point represents an individual spectrum and the data is restricted to ± 3 days from B_{max} . The fit applies to supernovae with $\Delta m_{15}(B) > 1.2$. For $\Delta m_{15}(B) < 1.2$ the line ratio is dominated by Si II and is not a good indicator of luminosity, decline rate or temperature.

5. Two for One: SN 1957A

The fecund NGC 2841 also produced SN 1957A which was identified as a subluminous type I supernova by Branch & Doggett (1985). Branch, Fisher, & Nugent (1993) describe it as a SN 1991bg-like event and a reanalysis of its photographic spectra by Casebeer et al. (2000) shows a flux deficit around 420 nm relative to normal SNIa at a similar age which suggests the presence of Ti II. However, in the blue part of the spectrum, a type Ic supernova can be mistaken for subluminous SNIa after maximum so SN 1957A can not be classified as a type Ia with absolute certainty. Still, we can analyze the historical light curve compiled by Leibundgut et al. (1991) as if it were a type Ia.

We fit the blue photographic light curve by stretching the Leibundgut template and find maximum occurred on Julian Day 2435901 ± 2 at $m_{pg} = 14.43 \pm 0.2$. The best fit stretch parameter is 0.54 ± 0.03 corresponding to a $\Delta m_{15}(B) = 2.00 \pm 0.07$. The V -band light curve is not as well sampled, so we use the same stretch factor and time of maximum to find a $V_{max} = 13.63 \pm 0.2$. The color of SN 1957A between 30 and 90 days from maximum is not

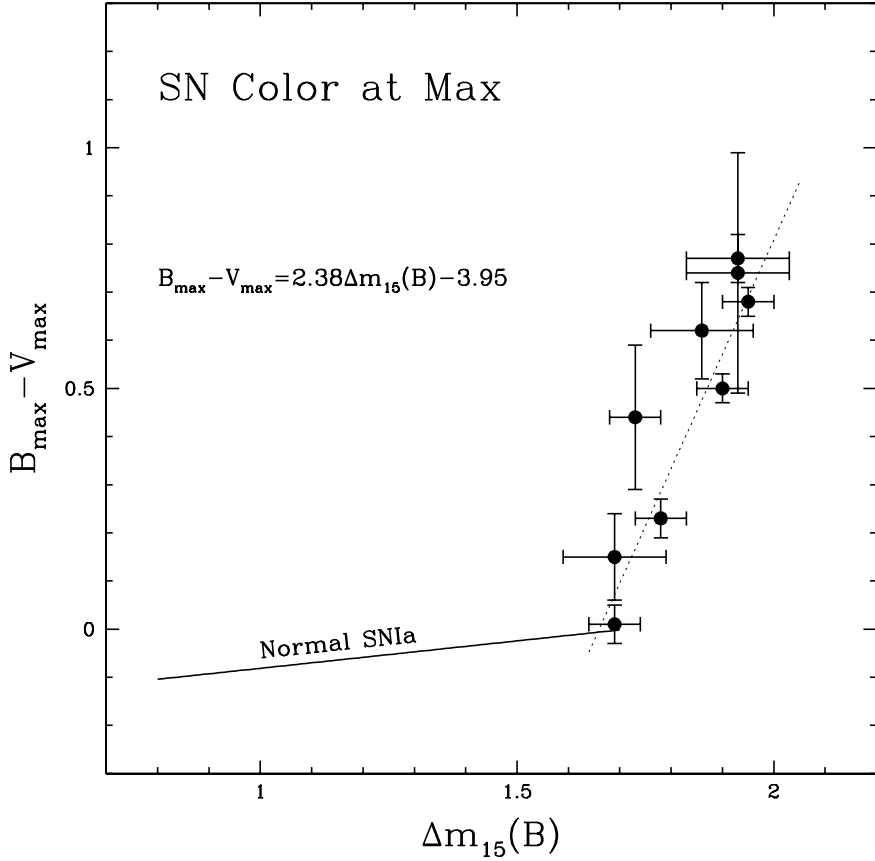


Fig. 15.— The $B_{max} - V_{max}$ color for SNIa. The line shows the color derived by Phillips et al. (1999) for normal SNIa.

very well determined given the errors on faint photographic magnitudes, so we will assume minimal extinction from the host. We convert between standard B -band and m_{pg} using equation 31 from Pierce & Jacoby (1995) and find SN 1957A was 0.88 mag fainter than SN 1999by in B and 0.48 mag fainter in V . If SN 1957A was truly an unreddened type Ia, then it was the faintest yet observed with $M_B = -16.3 \pm 0.2$ and $M_V = -17.2 \pm 0.2$. These are consistent with the luminosities predicted by equations 2 and 3 for $\Delta m_{15}(B) = 2.00$ of $M_B = -16.40$ and $M_V = -17.28$. The intrinsic color we find from the light curves of SN 1957A is $B_{max} - V_{max} = 0.87$ which is close to the 0.81 mag expected from its decline rate (see Figure 15).

6. The Hubble Constant

The measurement of a Cepheid distance to NGC 2841 provides an opportunity to make an independent estimate of the Hubble parameter using ‘peculiar’ SNIa alone. Jha et al. (1999) noted that most of the SNIa that have been calibrated with Cepheids have slow light

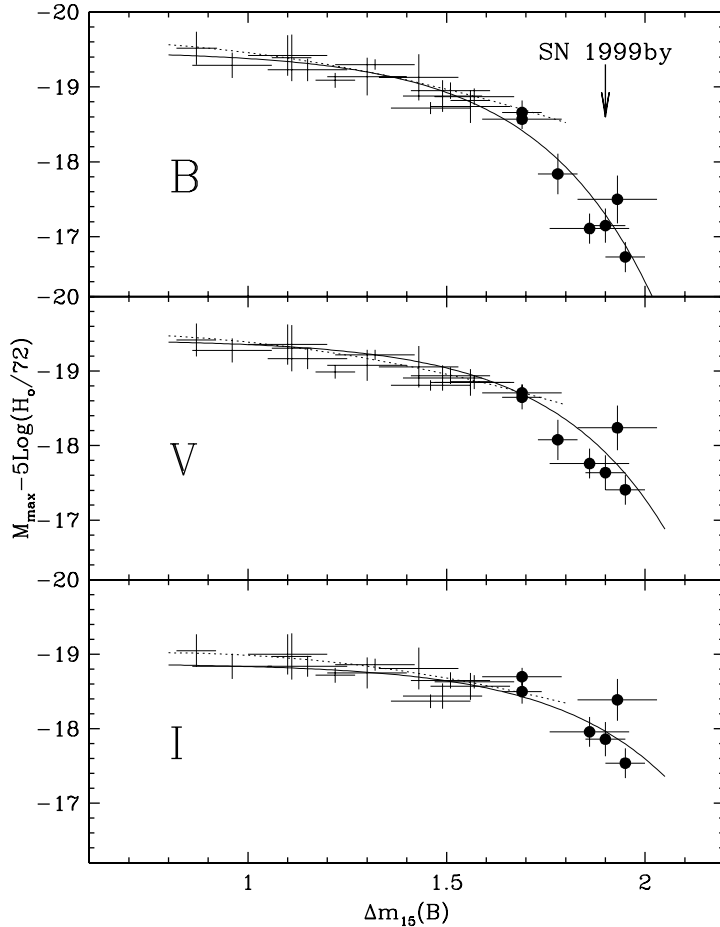


Fig. 16.— The absolute magnitudes of SNIa versus $\Delta m_{15}(B)$ from Phillips et al. (1999) with peculiar supernovae added (solid points). The dotted line is the quadratic fit derived by Phillips et al. for $\Delta m_{15}(B) < 1.7$. The solid line is an exponential fit which attempts to include normal and peculiar events.

curve decline rates. If there is a systematic bias caused by this selection, then the Hubble parameter estimated from fast-decliners may be significantly different from the Key Project value (Freedman et al. 2001). However, with only one calibrated peculiar supernova the uncertainty on the derived Hubble parameter can be no better than 10%.

There are only six SNIa listed in Table 5 that can be considered in the Hubble flow, that is with recession velocities in excess of 3000 km s^{-1} . We plot the luminosities of these in Figure 17 (assuming $H_0 = 72 \text{ km s}^{-1} \text{ Mpc}^{-1}$) as a function of $\Delta m_{15}(B)$. We also plot the luminosities versus $B_{max} - V_{max}$ because it appears to be highly correlated to the light curve shape in the fast-decliners. The slope of the linear fit to the points (excluding SN 1999by) is then used to estimate a magnitude correction to the fiducial values $\Delta m_{15}(B) = 1.90$ and $B_{max} - V_{max} = 0.50$. SN 1992K is consistently the most discrepant point from the linear trend and its errors in decline rate and peak brightness may be underestimated.

Using the method described in Jha et al. (1999), we derive a Hubble constant of

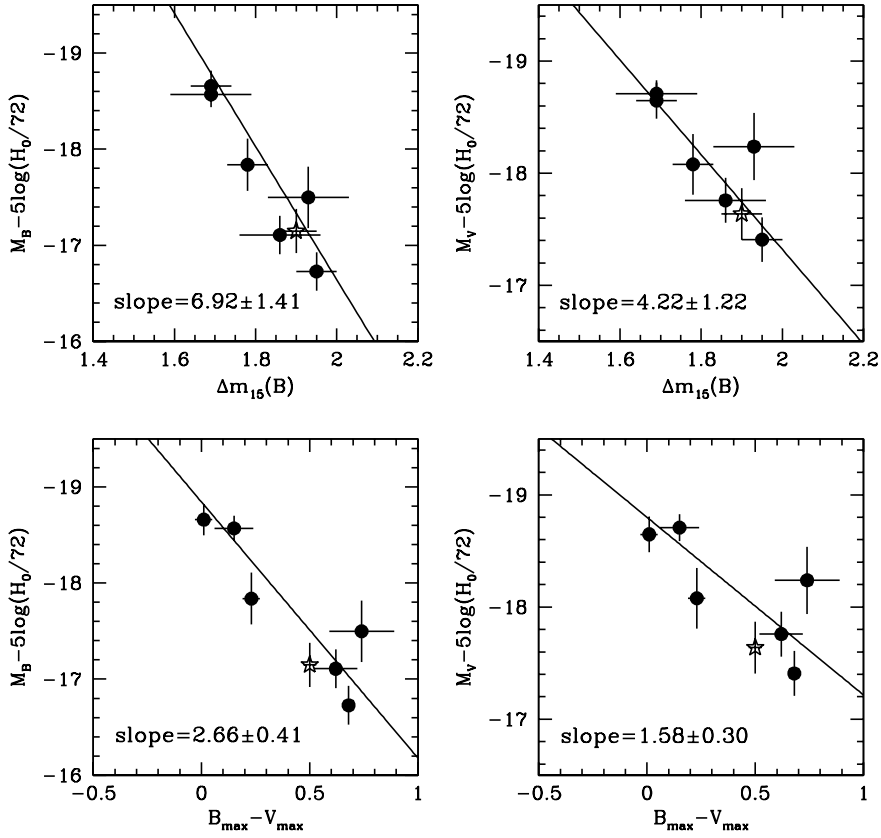


Fig. 17.— The absolute magnitudes of peculiar SNIa versus $\Delta m_{15}(B)$ and $B_{max} - V_{max}$. The star indicates the values for SN 1999by although it is not used in the linear fit.

$H_0 = 75_{-11}^{+12}$ km s $^{-1}$ Mpc $^{-1}$ applying the $\Delta m_{15}(B)$ parameter to correct the six events to SN 1999by. Using $B_{max} - V_{max}$ as the luminosity indicator, we find $H_0 = 84_{-11}^{+12}$ km s $^{-1}$ Mpc $^{-1}$. These are consistent with the Key Project value derived from normal SNIa (Freedman et al. 2001) and suggest that no systematic error in the Hubble constant is being introduced by ignoring low-luminosity events.

7. Conclusions

We present a well-sampled light curve of SN 1999by and the evolution of the spectra over a period of 40 days around maximum. We estimate a light curve parameter $\Delta m_{15}(B) = 1.90 \pm 0.05$ mag which is one of the fastest observed decline rates for a SNIa. The color at maximum $B_{max} - V_{max} = 0.50$ mag which is red for a SNIa, but the late-time color suggests little dust extinction along the line-of-sight. From the recent Cepheid distance to the host galaxy (Macri et al. 2001) and the assumption of minimal host extinction, we find the absolute brightness at maximum to be $M_B = -17.15 \pm 0.23$ and $M_V = -17.64 \pm 0.23$.

Comparing SN 1999by with other peculiar SNIa we find that it had a slower decline rate and was not as red at maximum as SN 1991bg or SN 1998de. It was slightly more luminous than SN 1998de, but fainter than SN 1998bp. There appears to be an excellent correlation between luminosity, decline rate and color for these subluminous objects and these observables blend smoothly into the luminous population of SNIa. We show that any SNIa with a decline rate of $\Delta m_{15}(B) < 2.0$ can be used as a distance indicator, although the scatter increases with large $\Delta m_{15}(B)$ due to the steep correction curve and poor calibration at the faint end of the population. We test this by using the ‘peculiar’ SNIa to estimate the Hubble constant and find it consistent with the value found from the ‘normal’ population.

We find that the 580 nm feature commonly associated with Si II and correlated with luminosity is actually dominated by Ti II for the SN 1991bg-like events and is likely to have a significant Ti II component even for more standard SNIa. This means that the depth ratio of 580 nm to 615 nm should not be used as a luminosity indicator for $\Delta m_{15}(B) > 1.2$, but it still makes an excellent temperature and luminosity estimator for supernovae with faster than normal light curves. Predictions of the Ti II strength with temperature suggest that Ti II optical depth increases rapidly over a small range of temperature. It is this non-linear effect that makes SN 1991bg-like events appear so odd when compared to more typical SNIa which change their character little over a wide temperature span. We conclude that SN 1991bg-like supernovae need not be considered as ‘peculiar’ SNIa since along with ‘Branch normal’ events they form a continuous, smooth, and single-valued distribution of luminosity, color and Ti II strength.

8. Acknowledgements

We thank the FLWO observers who helped gather these data: P. Berlind, N. Caldwell, M. Calkins, K. Dendy, E. Falco, D. McIntosh, M. Pahre, K. Rines, K. Stanek, A. Szentgyorgyi. The authors also thank T. Matheson for useful suggestions and discussions. We are grateful to the Vatican Observatory Research Group and R. Boyle for generous allotments of VATT nights. We also thank the NSF supported REU program at the Harvard-Smithsonian Center for Astrophysics. PMG was partially supported by NASA LTSA grant NAG5-9364 and RPK acknowledges support from NSF grant AST98-19825.

REFERENCES

Bonanos, A., Garnavich, P.M., Schlegel, E., et al. 1999, BAAS, 31, 1024

Branch, D. 2001, PASP, 113, 169

Branch, D., Fisher, A., & Nugent, P. 1993, AJ, 106, 2383

Cardelli, J.A., Clayton, G.C., & Mathis, J.S. 1989, ApJ, 345, 245

Casebeer, D., Branch, D., Blaylock, M., Millard, J., Baron, E., Richardson, D., & Ancheta, C. 2000, PASP, 112, 1433

Fabricant, D., Cheimets, P., Caldwell, N., & Geary, J. 1998 PASP, 110, 79

Filippenko, A.V., Richmond, M.W., Matheson, T., et al. 1992a, ApJ, 384, 15

Filippenko, A.V., Richmond, M.W., Branch, D., Gaskell, C.M., Herbst, W., Ford, C.H., Treffers, R.R., Matheson, T., Ho, L.C., Dey, A., Sargent, W.L., Small, T.A., & van Breugel, W.J.M. 1992b, AJ, 104, 1543

Filippenko, A.V. 1997, ARAA, 35, 309

Fisher, A., Branch, D., Hatano, K., & Baron, E. 1999, MNRAS, 304, 67

Freedman, W.L., et al. 2001, ApJ, 553, 47

Garnavich, P.M., et al. 1998, ApJ, 493, 53

Garnavich, P.M., Jha, S., & Kirshner, R.P. 1999, IAU Circ. 7159

Gerardy, C., & Fesen, R. 1999, IAU Circ. 7158

Goldhaber, G., et al. 2001, ApJ, in press, astro-ph/0104382

Hamuy, M., Phillips, M.M., Maza, J., Suntzeff, N.B., Della Valle, M., et al. 1994, AJ, 108, 2226

Hamuy, M., Phillips, M.M., Schommer, R.A., Suntzeff, N.B. & Maza, J., 1996a, AJ, 112, 2391

Hamuy, M., Phillips, M.M., Suntzeff, N.B., Schommer, R.A., Maza, J., et al. 1996b, AJ, 112, 2408

Hatano, K., Branch, D., Fisher, A., Baron, E., & Filippenko, A.V. 1999a, ApJ, 525, 881

Hatano, K., Branch, D., Fisher, A., Millard, J., & Baron, E. 1999b, ApJS, 121, 233

Hatano, K., et al. 2001, in preparation

Howell, D.A., Höflich, P., Wang, L., & Wheeler, J.C. 2001, astro-ph/0101520

Jha, S., Garnavich, P.M., Challis, P., & Kirshner, R.P. 1998, IAU Circ. 6891

Jha, S., Garnavich, P.M., Kirshner, R.P., et al. 1999, ApJS, 125, 73

Jha et al. 2001, in preparation

Landolt, A. 1992, AJ, 104, 340

Leibundgut, B., 1988, Ph.D. thesis, University of Basel

Leibundgut, B., Tammann, G.A., Cadonau, R., & Cerrito, D. 1991, A&AS, 89, 537

Leibundgut, B., Kirshner, R.P., Phillips, M.M., et al. 1993, AJ 105, 301

Li, W., Filippenko, A.V., Treffers, R.R., Riess, A.G., Hu, J., & Qiu, Y. 2001, ApJ, 546, 734

Lira, P., Masters thesis, Univ. of Chile.

Macri, L.M., Stetson, P.B., Bothun, G.D., Freedman, W.L., & Garnavich, P.M. 2001, *ApJ*, in press

Mazzali, P.A., Chugai, N., Turatto, M., Lucy, L.B., Danziger, I.J., Cappellaro, E., Della Valle, M., & Benetti, S. 1997, *MNRAS*, 284, 151

Modjaz, M., Li, W., Filippenko, A.V., King, J.Y., Leonard, D.C., Matheson, T., Treffers, R.R., & Riess, A.G. 2001, *PASP*, in press.

Nugent, P., Phillips, M., Baron, E., Branch, D., & Hauschildt, P. 1995, *ApJ*, 455, L147

Papenkova, M., Li, W.D., & Filippenko, A.V. 1999, *IAU Circ.* 7156

Perlmutter, S. et al. 1997, *ApJ*, 483, 565

Perlmutter, S. et al. 1999, *ApJ*, 517, 565

Phillips, M.M., Phillips, A.C., Heathcote, S.R., Blanco, V.M., Geisler, D., et al. 1987, *PASP*, 99, 592

Phillips, M.M., Wells, L. A., Suntzeff, N. B., Hamuy, M., Leibundgut, B., Kirshner, R. P., & Foltz, C.B. 1992, *AJ*, 103, 1632

Phillips, M.M. 1993, *ApJ*, 413, 105

Phillips, M.M., Lira, P., Suntzeff, N.B., Schommer, R.A., Hamuy, M., & Maza, J. 1999, *AJ*, 118, 1766

Pierce, M.J. & Jacoby, G.H. 1995, *AJ*, 110, 2885

Riess, A.G., Press, R.H., & Kirshner, R.P. 1995, *ApJ*, 438, 17

Riess, A.G., et al. 1998, *AJ*, 116, 1009

Riess, A.G., Filippenko, A.V., Li, W., Treffers, R.R., Schmidt, B.P., Qiu, Y., Hu, J., Armstrong, M., Faranda, C., Thouvenot, E., Christian, B. 1999a, *AJ*, 118, 2675

Riess, A.G., et al. 1999b, *AJ*, 117, 707

Schlegel, D.J., Finkbinder, D.P., & Davis, M. 1998, *ApJ*, 500, 525

Schmidt, B.P., et al. 1998, *ApJ*, 507, 46

Toth, I. & Szabó, R. 2000, *A&Ap*, 361, 63

Turatto, M., Benetti, S., Cappellaro, E., Danziger, I.J., Della Valle, M., Gouiffes, C., Mazzali, P.A., & Patat, F. 1996, *MNRAS*, 283, 1

Turatto, M., Piemonte, A., Benetti, S., Cappellaro, E., Mazzali, P.A., Danziger, I.J., Patat, F. 1998. *AJ*, 116, 2431

Vinkó, J., Kiss, L.L., Csák, B., Szabó, R., Thomson, J.R., & Mochnacki, S.W. 2001, *AJ*, accepted, *astro-ph/0103034*

Wells, L.A., et al. 1994, *AJ*, 110, 1440

Table 1. Local Standard Star Magnitudes

Star	<i>U</i>	<i>B</i>	<i>V</i>	<i>R</i>	<i>I</i>	n ^a
1	14.642	14.262	13.503	13.059	12.656	3
2	15.490	14.999	14.185	13.725	13.312	4
3	16.131	16.191	15.708	15.407	15.088	6
4	17.748	17.335	16.530	16.049	15.583	6
5	16.948	16.182	15.269	14.713	14.209	2
6	16.842	15.713	14.650	13.994	13.501	2
7	18.630	18.332	17.575	17.127	16.701	6
8	18.931	18.207	17.314	16.798	16.298	6
9	18.333	18.101	17.363	16.904	16.472	6
10	18.598	17.946	17.049	16.488	16.085	4

^aNumber of nights calibrated

Table 2. *UBVRI* Photometry of SN 1999by

Julian Date ^a	<i>U</i>	<i>B</i>	<i>V</i>	<i>R</i>	<i>I</i>	Observer
1304.67	13.959 (02)	13.947 (02)	13.643 (02)	13.487 (02)	13.404 (02)	Caldwell
1305.68	13.894 (02)	13.813 (02)	13.486 (02)	13.329 (02)	13.264 (02)	Caldwell
1306.67	13.842 (02)	13.738 (02)	13.373 (02)	13.198 (02)	13.141 (02)	Rines
1307.64	13.824 (02)	13.672 (02)	13.273 (02)	13.095 (02)	13.048 (02)	Rines
1308.63	13.837 (02)	13.656 (02)	13.207 (02)	13.019 (02)	12.986 (02)	Rines
1309.63	13.895 (02)	13.679 (02)	13.169 (02)	12.969 (02)	12.943 (02)	Rines
1310.73	13.993 (02)	13.716 (02)	13.136 (02)	12.940 (02)	12.908 (02)	McIntosh
1311.64	14.125 (03)	13.797 (02)	13.145 (02)	12.935 (02)	12.906 (02)	McIntosh
1312.70	14.297 (03)	13.923 (02)	13.175 (02)	12.953 (02)	12.904 (02)	Garnavich
1313.66	14.463 (03)	14.075 (02)	13.231 (02)	12.985 (02)	12.932 (02)	Dendy
1314.65	14.671 (03)	14.239 (02)	13.312 (02)	13.030 (02)	12.950 (02)	Dendy
1315.68	14.837 (03)	14.434 (02)	13.417 (02)	13.101 (02)	12.989 (02)	Dendy
1316.65	15.064 (04)	14.608 (02)	13.518 (02)	13.170 (02)	13.009 (02)	Pahre
1318.65	15.385 (05)	14.969 (02)	13.765 (02)	13.327 (02)	13.077 (02)	Pahre
1335.69	16.500 (07)	16.214 (03)	15.082 (03)	14.653 (03)	14.191 (03)	Szentgyorgyi
1338.66	16.572 (07)	16.327 (03)	15.208 (03)	14.813 (03)	14.361 (03)	Szentgyorgyi
1340.66	16.628 (07)	16.399 (03)	15.293 (03)	14.932 (03)	14.484 (03)	Szentgyorgyi
1342.67	16.715 (10)	16.452 (05)	15.374 (05)	15.029 (06)	14.593 (06)	Szentgyorgyi
1348.66	16.684 (15)	16.597 (08)	15.591 (06)	15.348 (09)	14.906 (09)	Falco
1350.65	16.772 (07)	16.665 (04)	15.651 (03)	15.423 (04)	15.000 (04)	Falco
1487.97	20.670 (30)	19.721 (05)	19.625 (05)	19.609 (05)	18.802 (05)	Stanek
1521.99	...	20.393 (20)	20.175 (12)	20.381 (20)	19.450 (30)	Garnavich

^a+2450000

Table 3. Log of Spectroscopic Observations

UT Date (1999)	JD	Coverage (nm)	Exposure	Observer
May 6	2451304.72	362-754	3×300	Berlind
May 7	2451305.63	362-754	2×660	Calkins
May 8	2451306.64	327-901	2×480	Calkins
May 9	2451307.64	362-560	600	Dendy
May 13	2451311.67	362-560	600	Dendy
May 14	2451312.64	327-940	3×480	Berlind
May 15	2451313.65	362-754	2×360	Berlind
May 16	2451314.67	362-754	2×420	Berlind
May 17	2451315.66	362-754	3×300	Garnavich
May 18	2451316.63	362-754	3×420	Garnavich
May 19	2451317.63	362-754	3×480	Garnavich
May 21	2451319.64	500-750	2×600	Calkins
May 22	2451320.64	390-595	2×600	Calkins
Jun 5	2451334.66	362-754	2×600	Calkins
Jun 9	2451338.66	362-754	2×600	Berlind
Jun 11	2451340.65	362-754	900	Calkins
Jun 13	2451342.65	362-754	900	Calkins
Jun 22	2451351.65	362-754	900	Calkins

Table 4. Light Curve Parameters

Band	JD Max	Obs. Max
<i>U</i>	2451307.6 ± 0.3	13.824 ± 0.03
<i>B</i>	2451308.8 ± 0.3	13.661 ± 0.02
<i>V</i>	2451310.8 ± 0.4	13.149 ± 0.02
<i>R</i>	2451311.4 ± 0.4	12.942 ± 0.02
<i>I</i>	2451311.8 ± 0.5	12.909 ± 0.03

Table 5. SN Ia with Fast-Declining Light Curves

SN	$\Delta m_{15}(B)$	cz	$B_0(\text{max})$	$V_0(\text{max})$	$I_0(\text{max})$	Reference
1992bo	1.69 (05)	5445 ^a	15.73 (07)	15.75 (06)	15.90 (05)	Hamuy et al. (1996)
1993H	1.69 (10)	7447 ^a	16.51 (08)	16.37 (05)	16.38 (06)	Hamuy et al. (1996)
1986G	1.73 (05)	547	9.90 (30)	9.46 (30)	...	Phillips et al. (1987)
1998bp	1.78 (05)	3127 ^a	15.29 (07)	15.06 (05)	...	Jha et al. (2001)
1997cn	1.86 (10)	5246 ^a	17.20 (10)	16.55 (10)	16.35 (10)	Turatto et al. (1998)
1999by	1.90 (05)	638	13.59 (03)	13.10 (03)	12.88 (03)	This work
1992K	1.93 (10)	3334 ^a	15.83 (21)	15.09 (16)	14.94 (15)	Hamuy et al. (1996)
1991bg	1.93 (05)	1060	14.58 (05)	13.82 (03)	13.50 (05)	Leibundgut et al. (1993)
1998de	1.95 (05)	4625 ^a	17.31 (04)	16.63 (04)	16.50 (05)	Modjaz et al. (2000)
1957A ^b	2.00 (07)	638	14.47 (20)	13.58 (20)	...	This work

^aCorrected to CMB frame

^bProbable type Ia